Charge stacking in the half-doped manganites

Z. Popović[a] and S. Satpathy[b]
Department of Physics and Astronomy, University of Missouri, Columbia, Missouri 65211

The stability of the charge-stacked structure vis-à-vis the charge-alternate structure in the half-doped manganites is studied with a model that includes electronic kinetic energy, onsite and intersite Coulomb interactions, the Jahn–Teller energy, and the antiferromagnetic superexchange between the manganese core spins. It is shown that for a single zigzag chain, the electronic kinetic energy stabilizes the standard chain, with Mn^{3+} at the bridge site and Mn^{4+} at the corner site, over the ''reversed'' zigzag chain with the two Mn valences interchanged. The electronic kinetic energy and magnetic interactions stabilize the three-dimensional charge-stacked structure, while a large intersite Coulomb interaction $V \geqslant V_c$ would stabilize the charge-alternate structure. It is argued that the magnitude of V is small enough that the charge-stacked structure is stabilized in the half-doped manganites such as $La_{1/2}Ca_{1/2}MnO_3$. © *2002 American Institute of Physics.*
[DOI: 10.1063/1.1456435]

A number of half-doped manganites such as $La_{1/2}Ca_{1/2}MnO_3$,[1] $Nd_{1/2}Sr_{1/2}MnO_3$,[2] $Pr_{1/2}Sr_{1/2}MnO_3$,[3] $Pr_{1/2}Ca_{1/2}MnO_3$,[4] $Nd_{1/2}Ca_{1/2}MnO_3$[5] etc., form in the so-called ''CE'' magnetic structure, which is well known from the pioneering works of Wollan and Koehler and of Goodenough in the 1950s.[6,7] The CE structure consists of ferromagnetic zigzag chains made up of alternating Mn^{3+} and Mn^{4+} charges, arranged antiferromagnetically on the basal planes. The planes are stacked one over the other, with neighboring planes having identical Mn charges but reversed magnetic moments, producing a charge stacked (CS) structure with lines of Mn^{3+} or Mn^{4+} extending normal to the planes.

A question of considerable interest is what stabilizes the charge-stacked structure in spite of the fact that it has the larger Coulomb energy. Even though in principle one should address this question from *ab initio* density-functional calculations of the total energy, given the complicated crystal structure, such studies are quite tedious, and even then one would need to develop models to understand the energetics involved. In view of this, in this paper we study the energetics of the charge stacked (CS) versus the charge-alternate (CA) structures from a model Hamiltonian that describes the interplay between the various competing interactions.

In our study, we considered three structures shown in Fig. 1: one CS structure (which is in fact the well known CE structure itself) plus two CA structures, which we call CA(1) and CA(2). Considering the structures as a collection of zigzag chains, we have two types of Mn sites: the bridge site A and the corner site B. In the observed CE structure in $La_{1/2}Ca_{1/2}MnO_3$ (denoted by CS in Fig. 1), the bridge sites are occupied by Mn^{3+} and the corner sites by Mn^{4+}, which we refer to as the standard zigzag chains. When the Mn valences are reversed, as in the $z=1/2$ plane of CA(1), we refer to those as reversed zigzag chains. We will subsequently show that these have higher energy as compared to the standard zigzag chains.

CA(1) has the same magnetic structure as CS, i.e., all nearest neighbor pairs of Mn moments are aligned in the same way (ferromagnetic or antiferromagnetic). However, on the consecutive planes of CA(1), Mn^{3+} alternates between the bridge site (A) and the corner site (B), forming zigzag

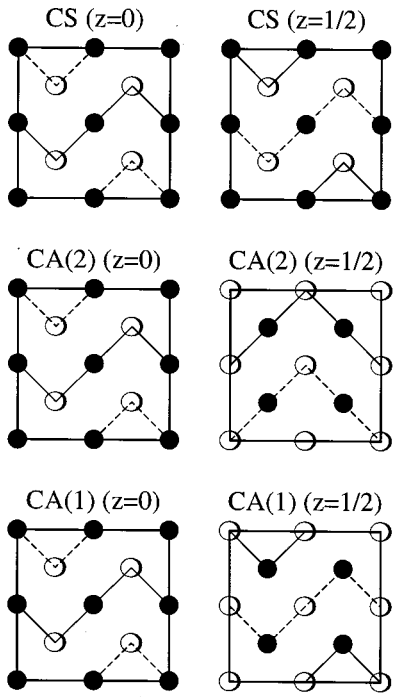

FIG. 1. Arrangement of the zigzag chains in the charge-stacked and the charge-alternate structures, CA(1) and CA(2), considered in the paper. Dashed and solid zigzag chains indicate opposite magnetic moments, while the full (open) circles indicate Mn^{3+} (Mn^{4+}) atoms. The CS structure is the same as the well-known CE structure. In all three structures, the $z=0$ and the $z=1/2$ planes are stacked alternately, one over the other. The $z=0$ planes are the same in all three structures. The $z=1/2$ plane may be obtained by a translation of the $z=0$ plane along the planar direction in CA(2), while in CA(1), the Mn valences are interchanged on the $z=1/2$ plane producing a plane of (reversed zigzag chains) with respect to the $z=0$ plane.

[a]Permanent address: Institute for Nuclear Sciences-''Vinča,'' P.O. Box 522, 11001 Belgrade, Yugoslavia.
[b]Electronic mail: satpathys@missouri.edu

chains and reversed zigzag chains on alternate planes, while in CS, all planes consist of standard zigzag chains. The CA(2) structure, obtained by shifting alternate planes of the CS structure with respect to one another, is the same as that considered by Yunoki *et al.*[8] Unlike CA(1), CA(2) has some unfavorable magnetic bonds. Comparing CA(1) and CA(2), CA(1) should have the better magnetic energy, while CA(2) should have the better kinetic energy (no reversed zigzag chains). The CS structure has both better magnetic energy and kinetic energy, but has a higher Coulomb energy due to charge stacking.

To study the energetics, we consider the following Hamiltonian describing the motion of the Mn(e_g) electrons on the underlying simple-cubic lattice with classical t_{2g} core spins fixed on the lattice sites:

$$\mathcal{H}=\mathcal{H}_{\rm kin}+\mathcal{H}_{\rm Coul}+\mathcal{H}_{\rm AF}, \tag{1}$$

with

$$\begin{aligned}\mathcal{H}_{\rm kin}&=\sum_{i\alpha\sigma}\epsilon_{i\alpha}n_{i\alpha\sigma}-J_H\sum_{i\alpha}\hat{S}_i\cdot\boldsymbol{\sigma}_{i\alpha}\\&\quad+\sum_{\langle i,j\rangle\alpha\beta,\sigma}t_{ij}^{\alpha\beta}(c_{i\alpha\sigma}^{\dagger}c_{j\beta\sigma}+\text{h.c.}),\\\mathcal{H}_{\rm Coul}&=U\sum_{i\alpha\beta,\sigma\sigma'}{}'\ n_{i\alpha\sigma}n_{i\beta\sigma'}+V\sum_{\langle ij\rangle}n_in_j,\\\text{and}\ \ \mathcal{H}_{\rm AF}&=J_{\rm AF}\sum_{\langle i,j\rangle}(\hat{S}_i\cdot\hat{S}_j+1).\end{aligned} \tag{2}$$

The first two terms are the kinetic and the Coulomb energies for the itinerant e_g electrons, while the last term is the antiferromagnetic superexchange between the t_{2g} core spins. Here $c_{i\alpha\sigma}^{\dagger}$ creates an e_g electron at site i with orbital α and spin σ, n is the number operator, U and V are, respectively, the onsite and the intersite Coulomb interactions, **S** is the classical t_{2g} core spin, $\langle ij\rangle$ denotes nearest-neighbors and the prime over the summation indicates exclusion of the self-interaction terms. $t_{ij}^{\alpha\beta}$ is the electronic tight-binding hopping integral between the e_g orbitals.[9]

The e_g basis set is chosen as follows: A1 is the "z^2-1" orbital with the local z axis along B-A-B on the zigzag chain, A2 is the corresponding "x^2-y^2" orbital, B1 is again the "z^2-1" orbital, but with the z axis normal to the planes, while B2 is the "x^2-y^2" orbital, with x,y axes pointing toward the A sites on the zigzag chain. For an isolated chain, A2 is not coupled to the rest of the e_g orbitals, within the nearest-neighbor tight-binding model.

The Jahn–Teller (JT) splitting $\Delta_{\rm JT}$ of the e_g orbitals is included in the onsite energy:

$$\epsilon_{i\alpha}=\pm(1/2)\Delta_{\rm JT}\times n_i, \tag{3}$$

taken proportional to the e_g electron occupancy n_i at site i. α denotes the two e_g orbitals, A1/A2 or B1/B2 at the respective sites. Thus the MnO_6 octahedral distortion responsible for the JT splitting is assumed to be possible at both sites, A or B, with equal ease. The splitting is dependent on the e_g occupation, being 0 for Mn^{4+} and $\Delta_{\rm JT}$ for Mn^{3+}. Unless otherwise stated, the sign of the JT interaction is chosen such that it splits A1 (B1) below A2 (B2), since in general this choice is found to have the lower energy. The following are typical parameters as obtained with guidance from the density-functional calculations:[10–13] $t_{dd\sigma}=-0.5$ eV, $\Delta_{\rm JT}=1$ eV, $J_H=2$ eV, $U=5$ eV, and $V\lesssim 0.05$ eV.

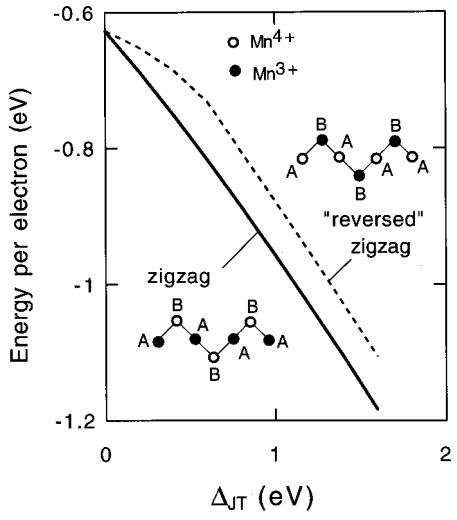

FIG. 2. Total energy of the 12-site zigzag chain obtained from exact diagonalization. The zigzag chain is energetically favored over the reversed zigzag chain. For the two chains, $\Delta_{\rm JT}$ is applied at the A and the B sites, respectively, in accordance with Eq. (4). Note that when $\Delta_{\rm JT}=0$, there is no difference between the two cases.

It is obvious that in the Hamiltonian (1), $J_{\rm AF}$ is **not** the net magnetic interaction between the core spins, since the itinerant e_g electrons produce a magnetic interaction as well, for instance, by the Anderson–Hasegawa mechanism, implicit in our Hamiltonian. The magnitude of $J_{\rm AF}$ is of the order of 10 meV, as estimated from the measured Neel temperature of ~110 K for $CaMnO_3$, which indicates $J_{\rm AF}\approx 7$ meV for that compound.[14]

We now consider the energetics of a single standard zigzag chain versus that of a reversed zigzag chain, both being ferromagnetic. The peculiarities of the electronic structure of a single zigzag chain have been recently examined by several authors.[13,15,16] For this calculation, we assume a JT distortion only at the A site (standard chain) or only at the B site (reversed chain), and use the expression

$$\epsilon_{i\alpha}=\pm(1/2)\Delta_{\rm JT} \tag{4}$$

for the JT sites instead of Eq. (3). At the non-JT sites, $\epsilon_{i\alpha}=0$.

The ground-state energy is obtained from exact diagonalization of the Hamiltonian (1), a method where the ground-state is expanded in terms of the many-particle configurations $|i\rangle$:$|G\rangle=\Sigma_i c_i|i\rangle$, and the resulting Hamiltonian matrix is diagonalized using the Lanczos method. We considered 12-site chains and the periodic boundary condition.

Results are shown in Fig. 2, which indicates the standard zigzag chain to have clearly the lower energy as compared to that of the reversed zigzag chain. The energy difference is primarily kinetic, due to the peculiarities of the tight-binding hopping and the chain geometry. For instance, we find that the energy difference between the standard and the reversed

chains is: $\Delta E = 89$ meV per e_g electron, with $t_{dd\sigma} = -0.55$ eV, $\Delta_{JT} = 0.8$ eV, $J_H = \infty$, $U = 5$ eV, and $V = 0$, while $\Delta E = 80$ meV with the same parameters except that $U = 0$, so that the Coulomb interaction does not produce much of a difference.

The important conclusion then is that it is energetically favorable for the system to have a JT distortion at the bridge site localizing the e_g electron there (standard zigzag chain) as opposed to having the same JT distortion at the corner site (reversed zigzag chain). This result is consistent with the occurrence of the standard zigzag chains in the CE structure.

In light of the above results, the CA(1) structure has higher energy than the other two within the isolated chain model, because half of the planes in CA(1) consist of reversed chains. When interchain interactions are included, interchain hopping as well as the intersite Coulomb and magnetic interactions come into play. Since the resulting 3D problem can no longer be solved accurately by exact diagonalization, we have solved it in the self-consistent Hartree–Fock approximation.

Now, the superexchange part in the Hamiltonian can be calculated by simply counting the number of bonds in Fig. 1. In fact, both CS and CA(1) have the same magnetic energy, all nearest-neighbor Mn moments being aligned the same way. In contrast, the CA(2) structure has half of its interplane bonds with ''wrong'' signs, being ferromagnetic instead of antiferromagnetic, costing an extra $2J_{AF}$ energy per e_g electron over the other two structures. This is added to our Hartree–Fock energies, which did not include the superexchange part.

The Hartree–Fock results including the superexchange part are shown in Fig. 3, taking $2J_{AF} = 40$ meV. With the parameters chosen, we see that if the intersite Coulomb V is zero, the CS structure has the lower energy while for a larger value of $V > V_c$, $V_c \sim 0.05$ eV, the CA(2) structure has the lower energy because of its lower Coulomb energy. The inset of Fig. 3 shows the charge order parameter,

$$\delta = n_A - n_B, \tag{5}$$

for the lowest-energy structure as a function of V. The intraplane charge order parameter δ_{xy} is defined as per Eq. (5) with both A and B atoms located on the same plane, while the interplane parameter δ_z corresponds to two atoms on the neighboring planes. The inset of Fig. 3 shows the transformation from charge stacking ($\delta_z \sim 0$) to charge alternation ($\delta_z \sim 1$), as V is increased.

The nearest-neighbor Coulomb interaction V may be expected to be quite small, given that there is an oxygen atom between the two Mn atoms producing considerable screening, and in light of our earlier estimates for Fe_3O_4, where $V \approx 0.05-0.1$ eV between two Fe atoms of comparable distances.[17] For the manganites, we expect the intersite Coulomb parameter V to be no more than 0.05 eV or so. With such a small V, the CS structure is stabilized over the CA structure because of the lower kinetic and magnetic energy of the former.

In conclusion, we have shown that the charge-stacked structure is favored over the charge-alternate structure because of its lower kinetic and magnetic energies, even though it has a higher Coulomb energy. More elaborate and realistic calculations such as density-functional calculations are needed to further understand the energetics.

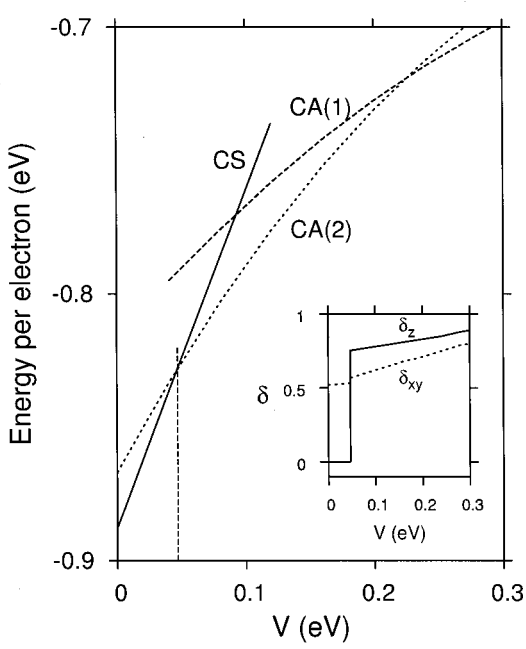

FIG. 3. Energetics of the charge-stacked and the charge-alternate structures. For $V \lesssim 0.05$ eV, the charge-stacked structure is energetically favorable, while for larger values, the charge-alternate structure, CA(1) or CA(2), has the lower energy. Inset shows the variation of the charge order parameters δ_{xy} and δ_z with V as the structure changes from CS to CA(2). The change is indicated by a sudden increase of the interplane charge-order parameter δ_z, which is zero for the CS structure but assumes a value of near unity for the CA structure.

This work was supported by the Department of Energy under Contract No. DOE FG02-00E0045818.

[1] Y. Okimoto *et al.*, Phys. Rev. Lett. **75**, 109 (1995); P. Schiffer *et al.*, *ibid.* **75**, 3336 (1995); P. G. Radaelli *et al.*, Phys. Rev. B **55**, 3015 (1997); S. Mori *et al.*, Nature (London) **392**, 473 (1998).
[2] H. Kuwahara *et al.*, Science **270**, 961 (1995); H. Kawano *et al.*, Phys. Rev. Lett. **78**, 4253 (1997).
[3] Y. Tomioka *et al.*, Phys. Rev. Lett. **74**, 5108 (1995).
[4] Z. Jirak *et al.*, J. Magn. Magn. Mater. **53**, 153 (1955); Y. Tomioka *et al.*, Phys. Rev. B **53**, R1689 (1996).
[5] T. Kimura *et al.* (unpublished).
[6] E. O. Wollan and W. C. Koehler, Phys. Rev. **100**, 545 (1955).
[7] J. B. Goodenough, Phys. Rev. **100**, 564 (1955).
[8] S. Yunoki, T. Hotta, and E. Dagotto, Phys. Rev. Lett. **84**, 3714 (2000).
[9] W. A. Harrison, in *Electronic Structure and the Properties of Solids* (Freeman, San Francisco, 1980).
[10] S. Satpathy, Z. S. Popović, and F. R. Vukajlović, Phys. Rev. Lett. **76**, 960 (1996); J. Appl. Phys. **79**, 4555 (1996).
[11] Z. S. Popović and S. Satpathy, Phys. Rev. Lett. **84**, 1603 (2000).
[12] W. E. Pickett, D. J. Singh, Phys. Rev. B **53**, 1146 (1996).
[13] Z. S. Popović and S. Satpathy, (preprint).
[14] H. Meskine, H. König, and S. Satpathy, Phys. Rev. B **64**, 094433 (2001), and references therein.
[15] I. V. Solovyev and K. Terakura, Phys. Rev. Lett. **83**, 2825 (1999).
[16] J. van der Brink, G. Khaliullin, and D. Khomskii, Phys. Rev. Lett. **83**, 5118 (1999).
[17] Z. Zhang and S. Satpathy, Phys. Rev. B **44**, 13319 (1991).